Pharm Res (2014) 31:3390–3403
DOI 10.1007/s11095-014-1429-9

RESEARCH PAPER

Characterization of Endogenous G-CSF and the Inverse Correlation to Chemotherapy-Induced Neutropenia in Patients with Breast Cancer Using Population Modeling

Angelica L. Quartino • Mats O. Karlsson • Henrik Lindman • Lena E. Friberg

Received: 19 January 2014 / Accepted: 3 June 2014 / Published online: 12 June 2014

ABSTRACT

Purpose Neutropenia is a severe adverse-event of chemotherapeutics. Neutrophils (ANC) are mainly regulated by granulocyte colony stimulating factor (G-CSF). The aim was to characterize the dynamics between endogenous G-CSF and ANC over time following chemotherapy.

Methods Endogenous G-CSF and ANC were monitored in forty-nine breast cancer patients treated with sequential adjuvant 5-fluorouracil–epirubicin–cyclophosphamide and docetaxel.

Results During treatment courses ANC was transiently decreased and was reflected in an endogenous G-CSF increase, which was well described by a semi-mechanistic model including control mechanisms; when G-CSF concentrations increased the proliferation rate increased and the bone maturation time reduced for ANC. Subsequently, ANC in the circulation increased leading to increased elimination of G-CSF. Additionally, a non-specific elimination for G-CSF was quantified. The ANC-dependent elimination contributed to 97% at baseline and 49% at an ANC of $0.1 \cdot 10^9$/L to the total G-CSF elimination.

Conclusion The integrated G-CSF–myelosuppression model captured the initial rise in endogenous G-CSF following chemotherapy-induced neutropenia and the return to baseline of G-CSF and ANC. The model supported the self-regulatory properties of the system and may be a useful tool for further characterization of the biological system and in optimization of chemotherapy treatment.

KEY WORDS breast cancer · chemotherapy · endogenous G-CSF · neutropenia · pharmacokinetics/pharmacodynamics (PKPD) modeling

ABBREVIATIONS

AAG	Alpha-1 acid glycoprotein
ALB	Albumin
ALT	Alanine aminotransferase
ANC	Absolute neutrophil count
ANC_0	Baseline neutrophil count
AP	Alkaline phosphate
AST	Aspartate aminotransferase
BSA	Body surface area
BSV	Between subject variability
CL_{CR}	Creatinine clearance
CRP	C-reactive protein
CV%	Coefficient of variation
$DOSE_{cort}$	Amount of cortisol-induced G-CSF release
FEC	5-flourouracil-epirubicin-cyclophosphamide
FOCE	First-order conditional estimation method
G-CSF	Granulocyte colony stimulating factor
$GCSF_0$	Baseline G-CSF
IL-6	Interleukin 6
k_{ANC}	ANC-dependent elimination rate constant
k_e	Non-specific elimination rate constant
MMT	Mean bone marrow maturation time of neutrophils
MMT_{FEC}	Mean bone marrow maturation time of neutrophils following FEC treatment
OFV	Objective function value
PK	Pharmacokinetics
PKPD	Pharmacokinetic-pharmacodynamic
rh-GCSF	Recombinant G-CSF
RSE	Relative standard error
$SLOPE_{5\text{-}FU}$	Linear drug effect parameters for 5-FU
$SLOPE_{cyclo}$	Linear drug effect parameters for 4-hydroxy cyclophosphamide

Electronic supplementary material The online version of this article (doi:10.1007/s11095-014-1429-9) contains supplementary material, which is available to authorized users.

A. L. Quartino (✉) · M. O. Karlsson · L. E. Friberg
The Pharmacometrics Research Group, Department of Pharmaceutical Biosciences, Uppsala University, Box 591, 75124 Uppsala, Sweden
e-mail: angelica.quartino@gmail.com

H. Lindman
Department of Oncology, Uppsala University Hospital, Uppsala, Sweden

$SLOPE_{doce}$	Linear drug effect parameters for docetaxel
$SLOPE_{epi,}$	Linear drug effect parameters for epirubicin
$t_{1/2}$ circ	Half-life of neutrophils in circulation
$t_{1/2}$ cort	Half-life of cortisol-induced G-CSF release
VPC	Visual predictive check
4-OHCP	4-hydroxy cyclophosphamide
5-FU	5-flourouracil
β	Feedback of G-CSF on transit time
γ	Feedback of G-CSF on neutrophil proliferation
$\theta_{MMT\text{-}doce}$	Change in MMT following docetaxel compared to FEC

INTRODUCTION

Neutropenia is a frequent and one of the most serious adverse events of chemotherapy as low neutrophil counts (ANC) increase the risk for life-threatening infections (1, 2). For patients with neutropenia the dose in the following cycle is reduced, delayed or both, which may lead to a sub-optimal cancer treatment (3). The main regulating factor of neutrophils is granulocyte colony stimulating factor (G-CSF) and is known to stimulate proliferation of the mitotic cells, to reduce the maturation time of the non-mitotic cells in the bone marrow and to prolong the life-span and enhance the function of mature neutrophils (4–6). G-CSF binds to the G-CSF receptor, which are located on cells in the whole neutrophil lineage with increasing number of receptors per cell, to exert its effects. Thereafter, the G-CSF-receptor complex is integrated and degraded (6). Thus G-CSF and neutrophils are affecting each other's kinetics and the plasma levels are inversely correlated (5–7). G-CSF is produced by different types of cells including macrophages, stromal cells in the bone marrow and endothelial cells and is triggered by inflammatory agents as well as by lipopolysaccharide released from bacteria (6, 8), which can result in highly increased levels of G-CSF e.g. one study showed an increase to 731.8±895.0 pg/mL in subjects with bacterial infection *vs* 25.3±19.7 pg/mL in healthy subjects (8).

Several mechanistic models for myelosuppression have been developed during the last 15 years (9, 10). Such models are valuable to describe the time-course of drug action and can be applied to predict different dosing scenarios. A frequently applied semi-mechanistic myelosuppression model, developed by Friberg *et al.*, (11) comprises of a proliferation compartment, representing the proliferating precursor cells in the bone marrow, that is linked via a chain of three transit compartments to a blood compartment. The transit compartments mimic the non-mitotic maturation of the neutrophils in the bone marrow and thereby reflect the delay seen between the drug action on proliferating precursor cells and the decrease of neutrophils in blood. The neutrophils randomly migrate from the blood to tissue and do not return. Chemotherapy induces killing of proliferative cells, while the non-mitotic cells are not affected. An empirical feedback mechanism, dependent on the ratio between the current and baseline ANC, is incorporated into the model to capture the stimulating effect of endogenous growth hormones, e.g. G-CSF, on the proliferation rate. A better understanding of the dynamics and interplay between endogenous G-CSF and neutrophils following chemotherapy could be used to improve the feedback mechanism of the model and thereby to increase its predictive capacity of different dosing strategies.

To our knowledge, no pharmacokinetic-pharmacodynamic (PKPD) model has been reported to describe the relationship between observed endogenous levels of G-CSF and ANC after treatment with chemotherapy. However, PKPD models of recombinant G-CSF (e.g. filgrastim, pegfilgrastim) and its effect on neutrophil production in healthy volunteers (12–17) and in patients (18, 19) have been proposed. The main elimination pathway of G-CSF in these models is the target-mediated clearance of G-CSF through binding to neutophils, which saturates at the high G-CSF concentrations achieved by labeled doses of recombinant G-CSF. The target-mediated clearance have been described by an empirical Michaelis-Menten function 12-15) or more mechanistically by linking the maximum elimination capacity to ANC (16), or by applying a target-mediated disposition model (17). The renal elimination of G-CSF, a linear elimination pathway, has been reported to be substantial and the reason for the short half-life for filgrastim (20, 21).

Since neutropenia is the most common dose-limiting toxicity of anticancer drug treatment it is important to increase the knowledge on how the neutrophil counts and the endogenous G-CSF levels interact and vary over time to improve the therapy for cancer patients. An integrated G-CSF-myelosuppression model describing this interaction may be valuable for optimization of chemotherapy and assist in identification of patients at high risk of severe neutropenia and thus in need of recombinant G-CSF.

The aim of this study was to conduct a prospective study to collect clinical data on the time-courses of endogenous G-CSF and ANC following adjuvant chemotherapy in early breast cancer patients, to 1) learn how endogenous G-CSF concentrations changes after treatment with chemotherapy; 2) characterize the relationship between endogenous G-CSF and ANC; 3) to evaluate the possibility of replacing the empirical feedback function in the semi-mechanistic myelosuppression model by Friberg *et al.* (11) by functions that depends on G-CSF concentrations.

MATERIAL AND METHODS

Study Design

A prospective observational study was conducted at the Department of Oncology, Uppsala University hospital,

Sweden, between February 2007 to January 2010. Patients were eligible for the study if they had breast cancer to be treated with adjuvant chemotherapy including docetaxel and/or epirubicin without any planned supportive treatment of recombinant G-CSF. The study was approved by the local ethics committee in Uppsala, Sweden (Dnr 2006/353) and all patients provided written informed consent before enrollment.

The choice of chemotherapy combination and dose adjustments was done at the physician's discretion (see result section for details). In general, the patients were treated according to standard adjuvant treatment at the Uppsala University hospital i.e. three cycles of the 5-flourouracil (5-FU)-epirubicin-cyclophosphamide (FEC) combination followed by 3 cycles of docetaxel given every 3 weeks. Typically FEC was administrated as a 1-h infusion of epirubicin followed by a 2-min infusion of 5-FU and a 15-min infusion of cyclophosphamide with median starting doses (cycle 1 and cycle 4) of 75 mg/m^2 (range 59–100 mg/m^2), 600 mg/m^2 (range 455–625 mg/m^2) and 600 mg/m^2 (range 455–625 mg/m^2), respectively and docetaxel was given as a 1-h infusion with a median starting dose of 80 mg/m^2 (range 61–104 mg/m^2). Doses were reduced by 20% in subsequent cycles if the patient experienced severe neutropenia ($<0.5 \cdot 10^9$ cells/L) for more than 1 week or if the next treatment cycle had to be delayed for two cycles in a row. The treatment was delayed if the absolute neutrophil count (ANC) was $<1.5 \cdot 10^9$ cells/L on the scheduled day of dosing.

Glucocorticoids were given to all patients. Betamethasone 8 mg was administrated 12 h before docetaxel treatment followed by 4 mg every 12 h for six doses (4 days). During FEC treatment betamethasone was administrated once a day for four consecutive days starting at the same day as FEC treatment with a dose of 4, 3, 2 and 1 mg for each respective day.

Blood Sampling

Blood samples for G-CSF were collected during treatment cycle one and four. Additional samples were drawn during cycle two for ten of the patients. Because the neutrophil nadir typically occurs at an earlier time point following docetaxel than following FEC, the sampling schedule depended on the treatment. Following docetaxel treatment samples were collected; predose and within the time intervals of day 5–8, 8–10, 10–15 and 18–22 while following epirubicin treatment samples were drawn predose and within the time intervals day 7–12, 12–14, 14–16 and 18–22. For the first 10 patients two extra blood samples per patient were drawn during the first treatment cycle according to predose, within the time intervals day 4–6, 6–8, 8–10, 10–13, 13–15 and 20–22 following docetaxel administration and predose, within the time intervals day 7–9, 9–11, 11–13, 13–15, 15–18 and 20–22 following FEC treatment. The actual time of sampling was recorded and used in the analysis. Blood samples were centrifuged within 30 min and the plasma aliquot was frozen at -70°C until analyzed.

Blood samples for differential white cell counts were collected concurrently with all G-CSF samples and, in addition, at predose and at expected nadir (day 7 post docetaxel administration and day 11 post FEC administration) for all other treatment cycles.

Additional laboratory tests including aspartate aminotransferase (AST), alanine aminotransferase (ALT), alkaline phosphate (AP), bilirubin, serum creatinine and plasma albumin (ALB) were recorded predose at each treatment cycle. The creatinine clearance (CL_{CR}) was calculated according to Cockcroft and Gault formula (22).

Bioanalytical Assay

G-CSF was analyzed using an ELISA assay (Quantikine™ Human G-CSF Immunoassay Kit, R&D systems, Inc., Minneapolis, MN). The lower limit of quantification of the assay was 15 ng/L plasma, but all values were retrieved and used in the data analysis. ANC and other laboratory measurements were analyzed according to standard routines at the central laboratory at Uppsala University hospital.

Data Analysis and Model Development

The data was analyzed by population (non-linear mixed effects) modeling approach where structural and variability parameters are estimated simultaneously. The model development was performed in three steps; 1) A semi-mechanistic model for myelosuppression (11) was applied to describe the ANC measurements and individual predictions of ANC were thereafter added to the dataset (using a 12 h interval); 2) A turn-over model for endogenous G-CSF was developed and the impact of target-mediated elimination of G-CSF was explored using the predicted ANC time-course; 3) A simultaneous analysis of ANC and G-CSF data was performed and the model structures for ANC and G-CSF were refined including substitution of the empirical feedback function regulating the neutrophil proliferation by functions of endogenous G-CSF.

Pharmacokinetic Models

Recorded covariates and dosing for each patient were used to drive published population PK models of docetaxel (23), FEC (24) and capecitabine (25) to generate individual plasma concentration-time profiles since no PK data was collected for the patients in the study. Docetaxel PK was generated by a three-compartment model with linear elimination covariates on clearance, i.e. body surface area (BSA), alpha-1 acid

glycoprotein (AAG), age, ALB and hepatic function (AST, ALT, AP) (23), The PK model for 5-FU consisted of a one-compartment model with capacity limited (Michaelis-Menten type) clearance (24). The included covariates were BSA on volume of distribution, and ALB and CL_{CR} on the elimination. Epirubicin followed a three-compartment disposition model with linear clearance that depended on the covariates ALB and bilirubin (24). The active metabolite of cyclophosphamide, 4-hydroxy cyclophosphamide (4-OHCP), was described by a two-compartment model with linear clearance which depended on ALB and BSA (24). The volume of distribution was influenced by ALT and body-weight. Capecitabine was described by a one-compartment model with first order absorption and a combined non-specific linear elimination and metabolic elimination. Capecitabine is transformed through metabolism into 5-FU (25).

Model for Neutropenia

The model was initially implemented as in the original publication (11) with the exception that the elimination of neutrophils from the circulation compartment to tissue was fixed to the literature value of neutrophil half-life of 7 h (26). Predicted drug concentrations in the central compartment were used to drive the drug effect on proliferative cells. To differentiate between the drug effects of the combination treatment, the previously reported estimate for epirubicin drug effect parameter ($SLOPE_{EPI}$) with its uncertainty (27) following FEC treatment was implemented as an informative prior (28) using the $PRIOR subroutine in NONMEM. Limited information was available for capecitabine and the drug-related parameter SLOPE was assumed to be the same as for its metabolite 5-FU. $SLOPE_{5\text{-}FU}$ was however estimated to zero, indicating it was not possible to separately quantify the drug effect of these compounds from the other chemotherapeutic drugs given in combination. For docetaxel, Emax and sigmoidal Emax models were also evaluated for the drug effect (11, 29), but a linear drug effect model was found to be sufficient to describe the data.

Model for G-CSF

One and two compartment disposition models were evaluated for G-CSF. The endogenous production of G-CSF was described by a constant zero-order production rate input equal to the product of baseline G-CSF and its elimination rate at steady state, i.e. when ANC is at baseline. Linear, power and Michaelis-Menten functions were tested for the non-specific and the neutrophil-dependent elimination pathways. The neutrophil-dependent elimination pathway was implemented as a function of the ANC in the circulating compartment or as a function of the whole neutrophil lineage (sum of all ANC compartments).

An input compartment was used to capture the temporarily increased production of G-CSF following betamethasone administration starting the evening prior to docetaxel administration The amount and half-life of the G-CSF release to the central G-CSF compartment were estimated. This approach was proposed by Ozawa *et al.* (30) and applied by Soto *et al.* (31) to describe the temporarily increase in ANC following dexamethasone treatment. A more sophisticated model describing the influence of cortisol on the dynamics of G-CSF would be difficult to implement as the exact time and dose of betamethasone administration or betamethasone concentrations were not recorded. This increased release of G-CSF explained the relatively high G-CSF observations in the samples collected on the day of docetaxel administration. As doses of betamethasone in the FEC regimen were lower and the time between betamethasone dosing and the G-CSF and ANC samples were substantially longer (2–4 days compared to 12 h) it was assumed that their impact on the observed G-CSF was negligible. This assumption is supported by the fact that there was no residual effect on G-CSF levels of high doses of dexamethasone given in healthy males after 3–4 days (32) as well as no apparent visible increase of ANC after a few days following dexamethasone in patients or corticosteroids in healthy volunteers (30, 33).

Between Subject and Residual Error Model

Between subject variability (BSV) was evaluated on all the model parameters for its significance and was assumed to be log-normally distributed. Potential correlations between parameters were investigated using the covariance matrix for random effects.

The ANC were Box-Cox-scale transformed with a lambda (λ) of 0.2 (34, 35) according to Eq 1 and the residual error was modeled as an additive error on the Box-Cox scale.

$$ANC_{BOX-COX} = \frac{ANC^{\lambda} - 1}{\lambda} \quad (1)$$

The G-CSF levels were log-transformed during the analysis and the residual error was described by a proportional and an additive component. The need for a separate residual error for observations below the quantification limit was also evaluated for G-CSF as these measurements are potentially quantified with a higher imprecision, but was not significant.

Model Evaluation

The final model was evaluated using internal validation procedures. A stratified nonparametric bootstrap was performed to assess the uncertainty of the parameter estimates. The patients were stratified based on the sampling schedules i.e. patient 1–10, 11–20 and 21–50 and number of bootstrap samples was

limited to 40 due to long run times. The visual predictive check (VPC) was used to assess the predictive performance of the model. Simulations were performed ($n=500$) using the model and the original dataset as a template and 95% confidence intervals were computed for the 10th, median and 90th percentiles based on the simulated data. The model was considered to perform well if the confidence intervals included the corresponding percentiles of the observed data.

Software and Methodology

The non-linear mixed effects modeling was carried out using the software NONMEM 7.1.2 (36), and the first-order conditional estimation (FOCE) method with interaction. The software PsN (http://psn.sourceforge.net/) was used for executing estimations as well as for simulations and calculations for the VPC. Graphical assessment of the model fit was performed using Xpose 4 (http://xpose.sourceforge.net/) implemented in R (http://www.r-project.org/).

Model development was guided by the objective function value (OFV) and precision in parameter estimates (relative standard error RSE %) as well as graphical assessments and knowledge of the physiological system. To differentiate between two nested models a log-likelihood ratio test of the OFV obtained from NONMEM was used. The difference in OFV between two nested models is approximately χ^2-distributed and a decrease in OFV of 10.83 for one extra parameter corresponds to $p<0.001$, which was considered significant.

RESULTS

Patients

Fifty early breast cancer patients enrolled in the study of which 49 patients completed the study (one patient withdrew the informed consent). One patient stopped the treatment after five treatment cycles due to cardiovascular toxicity. Most patients ($n=39$) received the standard FEC (3 cycles) followed by docetaxel (3 cycles). Six patients received the treatments in opposite order; two patients were treated with six cycles of FEC; one patient received three cycles of FEC, two cycles of docetaxel and then one cycle of FEC; and one patient received three cycles of docetaxel followed by three cycles of epirubicin, cyclophosphamide and capecitabine (3,500 mg/day during day 1-14 of each treatment cycle). Five patients received recombinant G-CSF (rh-GCSF; Neulasta®) during one or several treatment cycles during cycle 2–6 after experiencing severe neutropenia in a previous cycle. Data collected up to their first dose of rh-GCSF was included in the analysis (1–4 cycles per patient). Data after the first administration of rh-GCSF was excluded as the data were too limited to support characterization of rh-GCSF dynamics as part of the model.

Baseline patient characteristics are presented in Table I. In the analysis, a total of 967 ANC (range 11–27 per patient) and 514 G-CSF (range 4–15 per patient) measurements from 49 patients were included.

Endogenous G-CSF and ANC

The time-course of observed ANC and endogenous G-CSF measurements superimposed with the corresponding prediction of the final integrated G-CSF-myelosuppression model is shown in Fig. 1. During treatment ANC was transiently decreased and was reflected in an endogenous G-CSF increases following chemotherapy in patients with early breast cancer thus the two are inversely correlated with each other.

The baseline G-CSF concentration for docetaxel was substantially higher than for FEC, as a result of differences in betamethasone administration for docetaxel and FEC. High variability in endogenous G-CSF concentrations was observed between patients but also between treatment cycles within a

Table I Baseline Patient Characteristics

	Median	Range
Demographics		
Age, years	54	31–73
Body-weight, kg	70	54–111
Body surface area, m^2	1.80	1.5–2.2
Laboratory tests		
s-ALT, μcat/L	0.43	0.16–1.63
s-AST, μcat/L	0.39	0.20–0.88
s-AP, μcat/L	1.15	0.50–2.90
s-Bilirubin, μmol/L	8	4–16
s-Albumin g/L	39	33–47
s-creatinine, μmol/L	64	42–103
CLcr, mL/min[a]	106	51–177
	No. of patients	Relative frequency (%)
ECOG PS 0	49	100
Menopausal status -pre	20	41
Menopausal status -post	29	59
Elston Grade		
1	1	2
2	17	35
3	31	31
Ductal breast cancer	47	96
Lobular breast cancer	2	4
ER – positive	37	76
PGR –positive	35	71
HER-2 positive	10	20

AST, aspartate aminotransferase; *ALT*, alanine aminotransferase; *AP*, alkaline phosphate; *s*, serum; *CLcr*, creatinine clearance; *ECOG PS*, Eastern cooperative oncology group performance status

[a] According to Cockroft and Gault, based on total body weight

patient. This variability was largely explained in the model by predicted neutrophil counts.

The final integrated G-CSF-myelosuppression model captured both the initial rise in endogenous G-CSF concentrations following chemotherapy-induced neutropenia and the subsequent return to baseline for G-CSF and ANC. The final model structure is illustrated in Fig. 2 and the NONMEM code is provided in Supplementary material 1.

Model for Neutropenia

A semi-mechanistic myelosuppression model (see introduction) (11) initially used to describe the time-course of ANC following chemotherapy, included three system-related parameters; baseline neutrophil count (ANC_0), mean bone maturation time (MMT) and the empirical feedback factor on ANC proliferation (γ) and one drug specific parameter (SLOPE). The elimination of neutrophils from the circulation compartment to tissue was fixed to the literature value of neutrophil half-life of 7 h ($=LN(2)/k_{circ}$) (26). The drug-related effect (E_{DRUG}) was expressed as a linear function dependent on the drug concentration (C) and the drug specific parameter (SLOPE). The total drug effect for combination treatments was assumed to be additive according to Eq. 2.

$$E_{DRUG} = SLOPE_{5-FU} \bullet C_{5-FU} + SLOPE_{epi} \bullet C_{epi} + SLOPE_{4OHCP} \bullet C_{4OHCP} + SLOPE_{cape} \bullet C_{cape} + SLOPE_{doce} \bullet C_{doce} \quad (2)$$

Information on patient covariates and dosing were used to drive published population PK models of docetaxel (23), FEC (24) and capecitabine (25) to generate plasma concentration-time profiles since no individual PK data was collected for the patients in this study. Between subject variability was evaluated for each of the SLOPE parameters. A common BSV parameter for epirubicin and 4-hydroxy cyclophosphamide was equally good (no difference in OFV) as separate variability parameters for the two drugs. Variability in docetaxel drug effect was low (10%) when the semi-mechanistic myelosuppression model was fitted to the ANC measurements alone; and when ANC and G-CSF data was analyzed simultaneously BSV in SLOPE was no longer statistically significant for docetaxel and was therefore omitted from the final model. No significant correlation was found between docetaxel and FEC SLOPEs and thus, as expected, a common BSV parameter for docetaxel, epirubicin and 4-hydroxy cyclophosphamide SLOPEs resulted in a worse model fit.

In the final integrated G-CSF-myelosuppression model the semi-mechanistic myelosuppression model was modified by; 1) using four transit compartments instead of three to describe the ANC maturation time-course (OFV decreased 34 units). The MMT was treatment dependent and was estimated to be 210 h for FEC and 133 h for docetaxel (OFV decreased 236 units); 2) replacing the empirical feedback mechanism on neutrophil proliferation by functions of G-CSF. Eqs., 3–12 describes the final model, where n is the number of transit compartments.

$$\frac{dANC_{Prol}(t)}{dt} = k_{prol} \bullet ANC_{Prol}(t) \bullet (1 - E_{DRUG}) \bullet FB_{kprol} - k_{tr} \bullet ANC_{Prol}(t) \bullet FB_{ktr} \quad (3)$$

$$\frac{dANC_{TR1}(t)}{dt} = k_{tr} \bullet ANC_{Prol}(t) \bullet FB_{ktr} - k_{tr} \bullet ANC_{TR1}(t) \bullet FB_{ktr} \quad (4)$$

$$\frac{dANC_{TRi}(t)}{dt} = k_{tr} \bullet ANC_{TRi-1}(t) \bullet FB_{ktr} - k_{tr} \bullet ANC_{TRi}(t) \bullet FB_{ktr}, i = 2, \ldots, 4 \quad (5)$$

$$\frac{dANC_{Circ}(t)}{dt} = k_{tr} \bullet ANC_{TRn}(t) \bullet FB_{ktr} - k_{circ} \bullet ANC_{Circ}(t) \quad (6)$$

$$FB_{kprol} = \left(\frac{GCSF_{Circ}}{GCSF_0}\right)^{\gamma} \quad (7)$$

$$FB_{ktr} = \left(\frac{GCSF_{Circ}}{GCSF_0}\right)^{\beta} \quad (8)$$

$$\text{MMT} = \frac{n+1}{k_{tr}} \quad (9)$$

$$ANC_{Prol}(0) = \frac{ANC_0 \bullet k_{circ}}{k_{tr}} \quad (10)$$

$$ANC_{TRi}(0) = \frac{ANC_0 \bullet k_{circ}}{k_{tr}} i = 1, \ldots, 4 \quad (11)$$

$$ANC_{Circ}(0) = ANC_0 \quad (12)$$

Two of G-CSF's effects on ANC were incorporated into the model. The first one was the control of the proliferation rate of ANC (Eq 7). An additional feedback mechanism (Eq. 8), in which increased G-CSF levels reduced MMT, further improved the model fit to the data (OFV decreased 115 units). The G-CSF functions resulted in a better model fit

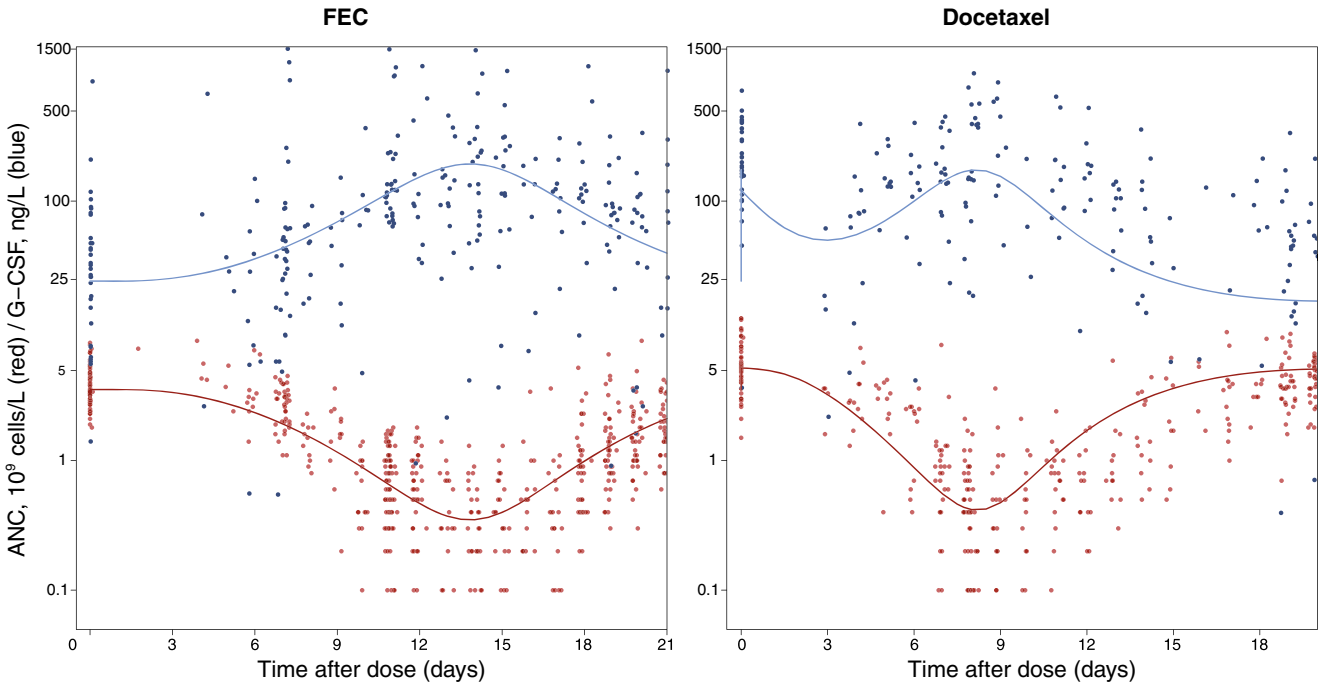

Fig. 1 Observed individual profiles of endogenous G-CSF (*blue*) and neutrophils (*red*) following FEC (*left*) and docetaxel (*right*) treatment. The model prediction of a typical patient following corresponding treatments is shown in solid lines.

(OFV 31 units lower) compared to the corresponding model with empirical functions on the proliferation rate and maturation time. A comparison between the two feedback functions shows that the amplitude is larger for the G-CSF feedback than the empirical function (Fig. 3). It was also observed that the feedback amplitude is larger following FEC treatment (course 1–3) than docetaxel treatment (course 3–6). The amplified feedback due to increase in G-CSF

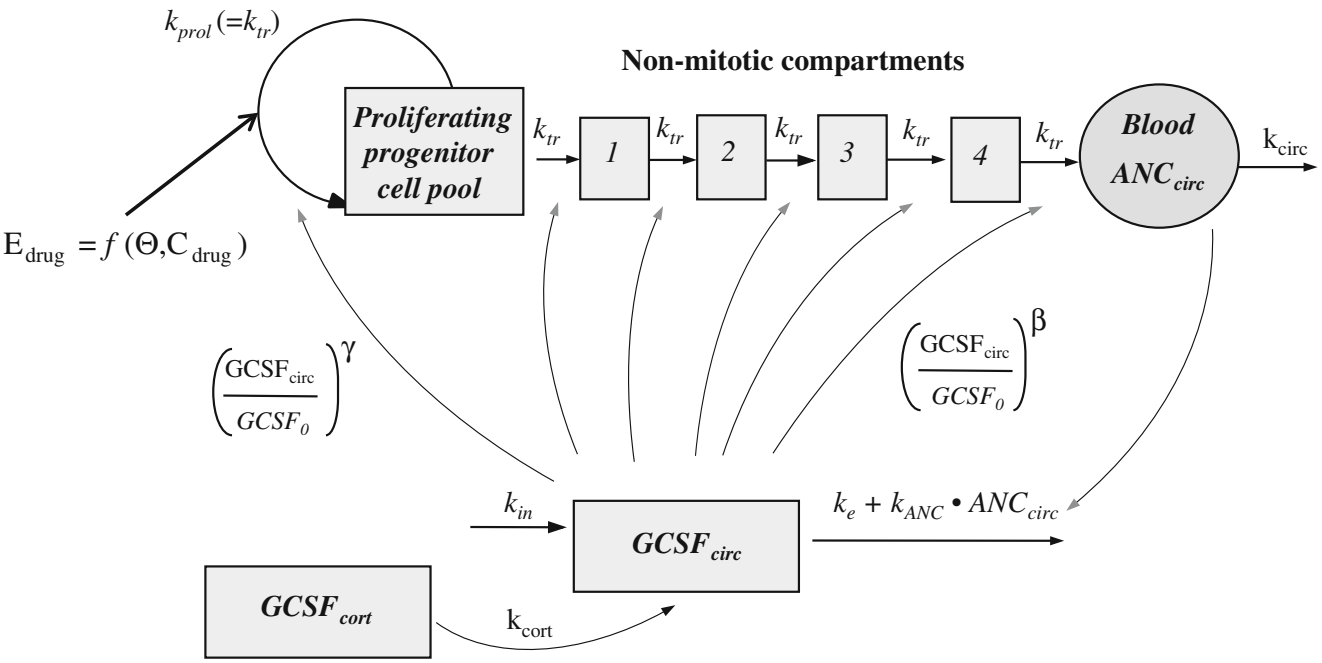

Fig. 2 The integrated G-CSF-myelosuppression model describing the dynamics of endogenous G-CSF and neutrophils following chemotherapy. For the myelosuppression model the parameters are baseline neutrophil count (ANC_0), mean maturation time ($MMT = 5/k_{tr}$), the half-life of neutrophils in circulation ($t_{½circ} = LN(2)/k_{circ}$), the feedback parameters of G-CSF on neutrophil proliferation (γ) and transit time (β) and the drug related effect (E_{drug}). The estimated parameters for the G-CSF turnover model are baseline G-CSF ($GCSF_0$), nonspecific elimination rate constant (k_e) and ANC-dependent elimination rate constant (k_{ANC}) and cortisol-induced G-CSF release ($DOSE_{cort}$) and the half-life of cortisol-induced G-CSF release ($t_{1/2\ cort} = LN(2)/k_{cort}$).

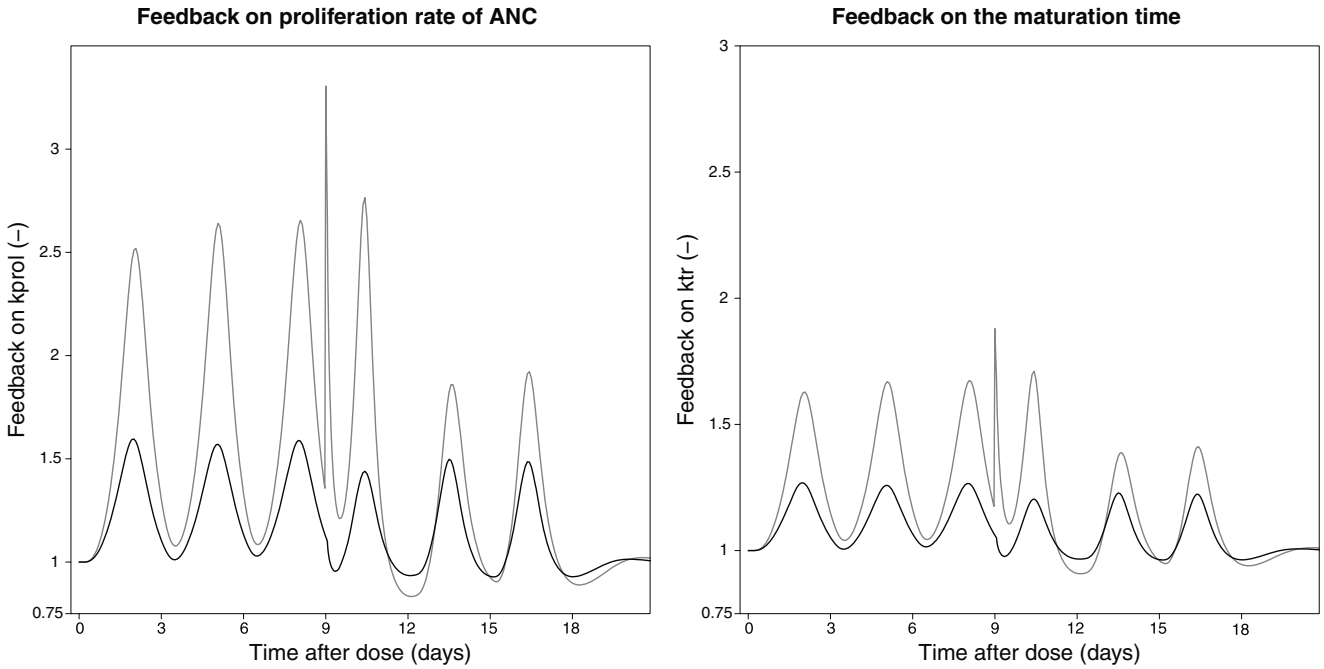

Fig. 3 Comparison of the feedback function given the original empirical function (*black*) and the G-CSF driven function (*grey*) for a typical patient receiving sequential treatment of three courses of FEC followed by three courses of docetaxel. The feedback on the proliferation rate (*left*) and the feedback on the transit time in bone marrow (*right*).

following glucocorticoid administration is apparent at the third treatment cycle at week 9.

Model for Endogenous G-CSF

The endogenous G-CSF concentrations were described by a one compartment turnover model with a zero-order production rate (k_{in}, (ng/L)/h). The elimination was described by a combined non-specific linear elimination (k_e, h^{-1}) and a neutrophil-dependent elimination (k_{ANC}, h/[10^9 cells/L]), which was proportional to the number of neutrophils in the blood circulation. Non-linear functions of the elimination were explored but were not supported by the data. In addition, since G-CSF is known to bind to receptors on neutrophils in the whole maturation lineage, a model where the neutrophil-dependent elimination was a function of the sum of all ANC compartments instead of the neutrophils in blood circulation was also tested; however this model resulted in a significantly worse fit to the data (OFV increased 68 units).

A rapid increase in G-CSF following betamethasone administration prior to docetaxel administration was evident by the higher pre-dose G-CSF values compared to pre-dose values for FEC treatment. The corticosteroid effect was explained by a temporarily increase in G-CSF production modeled as a one compartment model including an initial estimated G-CSF amount equal to the parameter $DOSE_{cort}$ which was subsequently released into the G-CSF plasma compartment with an estimated half-life of $t_{1/2\ cort}$ (=LN(2)/k_{cort}). Addition of this input compartment resulted in a substantial improvement in model fit (OFV decreased 145 units).

The endogenous G-CSF concentration (ng/L) was described by Eqs. 13–17.

$$\frac{dGCSF(t)}{dt} = k_{in} - (k_e + k_{ANC} \times ANC(t))k_{cort} \times GCSF_{cort}(t) \tag{13}$$

$$k_{in} = GCSF_0 \times (k_e + k_{ANC} \times ANC_0) \tag{14}$$

$$\frac{dGCSF_{cort}(t)}{dt} = -k_{cort} \times GCSF_{cort}(t) \tag{15}$$

$$GCSF(0) = GCSF_0 \tag{16}$$

$$GCSF_{Cort}(0) = 0 \tag{17}$$

Model Evaluation

The final integrated G-CSF-myelosuppression model was evaluated using VPCs stratified by treatment (Fig. 4) and showed that simulations from the model adequately match the observed data. The higher baseline G-CSF concentrations in cycles with docetaxel treatment, compared to cycles with

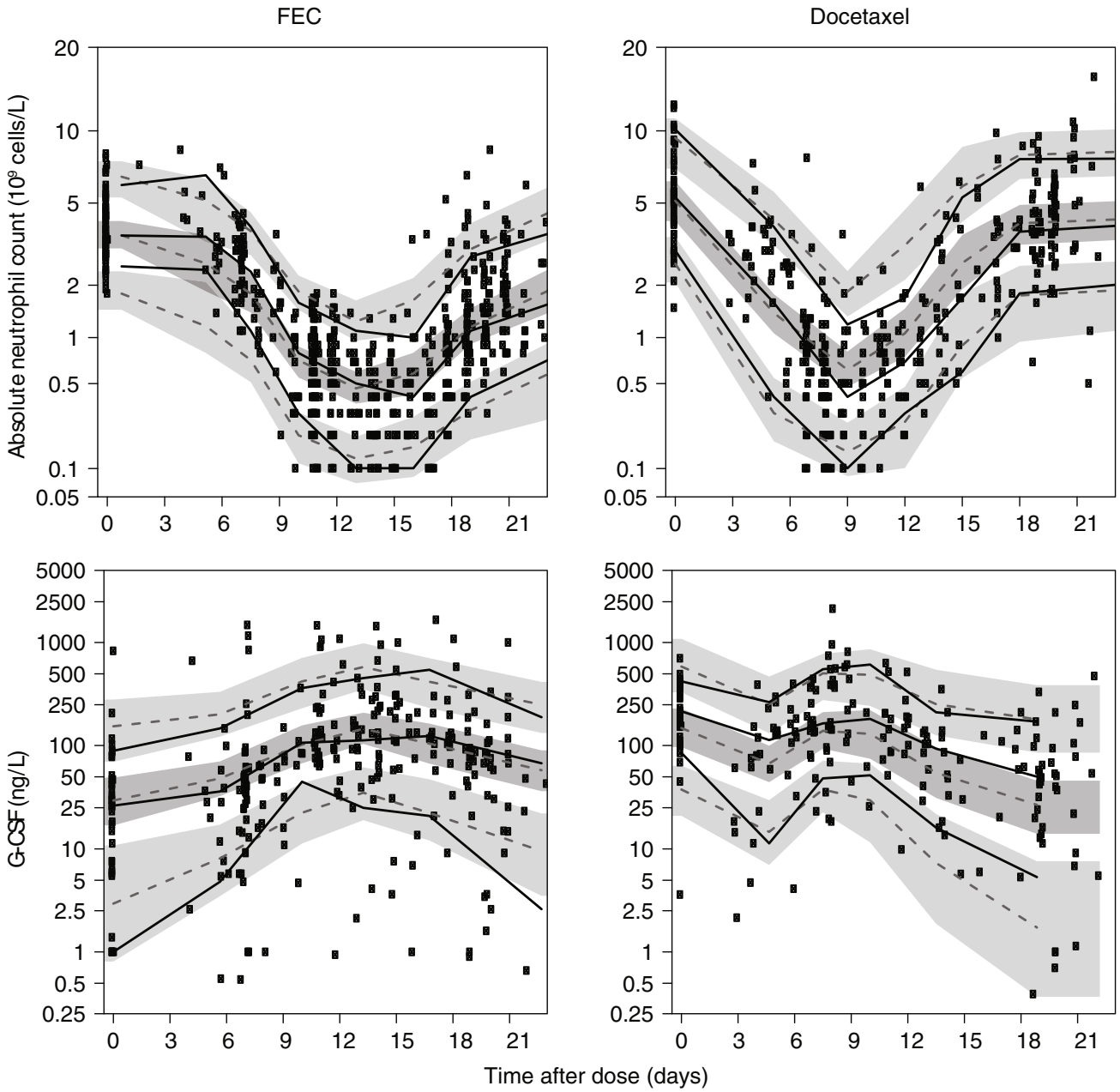

Fig. 4 Visual predictive check (80% prediction interval) of the integrated G-CSF-myelosuppression model for neutrophils (*top*) and endogenous G-CSF (bottom) following administration of FEC (*left*) and docetaxel (*right*). Observed data (*dots*) and the 95% confidence intervals of the simulated median (*grey*), and the 10th and 90th percentiles (*light grey*) are shown. Solid and dotted lines are the corresponding median and percentiles, respectively, of the observed data (*black*) and simulated data (*grey*).

FEC treatment, were also well captured by the model, and was explained by the high dose betamethasone administered 12 h prior docetaxel dosing. The model slightly under-predicts the G-CSF at baseline and ANC around day 9 for docetaxel treatment. The model parameters (Table II) were estimated with reasonable precision (relative standard errors ≤36%). Between-subject variability in G-CSF were in the final model included for two of the parameters; $GCSF_0$ (68%) and k_{ANC} (106%). Individual model predictions of endogenous G-CSF and ANC for a set of randomly selected patients show that the model was able to describe the time-courses following chemotherapy for most patients (Fig. 5).

DISCUSSION

Time-course of endogenous G-CSF concentrations and ANC were quantified in a prospective clinical study in early breast cancer patients treated with adjuvant chemotherapy consisting of three courses of FEC followed by 3 courses of

Table II Parameter Estimates of the Final G-CSF-Myelosuppression Model

	Typical estimate (% RSE)		BSV, CV% (% RSE)	
ANC_0 ($\bullet 10^9$ cells/L)	3.53	(5)	23	(16)
$t_{1/2}$ circ (h)	7 FIXED	(−)		
MMT_{FEC} (h)	210	(2)	12	(13)
$\theta_{MMT\text{-}doce}$ (−)	−0.366[a]	(6)		
γ (−)	0.444	(4)		
β (−)	0.234	(8)		
$SLOPE_{doce}$ (L/μmol)	17.2	(4)		
$SLOPE_{epi}$ (L/μmol)	22.0	(16)	14[b]	(23)
$SLOPE_{4OHCP}$ (L/μmol)	5.99	(19)	14[b]	(23)
$SLOPE_{5\text{-}FU}$ (L/μmol)	0 FIXED	(−)		
Additive residual error on Box-Cox scale (−)	0.572	(5)		
$GCSF_0$ (ng/L)	24.3	(8)	68	(12)
k_e (h^{-1})	0.592	(32)		
k_{ANC} (h/(10^9 cells/L))	5.64	(25)	106	(31)
$DOSE_{cort}$ (μg/L)	99.4	(36)		
$t_{1/2}$ cort (h)	25.5	(7)		
Proportional residual error (%)	73	(8)	22	(30)
Additive residual error (ng/L)	22	(24)		

ANC_0, baseline neutrophil count; *$t_{1/2}$ circ*, half-life of neutrophils in circulation; *MMT_{FEC}*, mean maturation time of neutrophils following FEC; *$\theta_{MMT\text{-}doce}$*, change in MMT following docetaxel compared to FEC; *γ*, feedback of G-CSF on neutrophil proliferation; *β*, feedback of G-CSF on transit time; *$SLOPE_{doce}$*, *$SLOPE_{epi}$*, *$SLOPE_{cyclo}$*, *$SLOPE_{5\text{-}FU}$*, linear drug effect parameters for docetaxel, epirubicin, 4-hydroxy cyclophosphamide and 5-FU; *$GCSF_0$*, baseline G-CSF; *k_e*, non-specific elimination rate constant, *k_{ANC}* ANC-dependent elimination rate constant; *$DOSE_{cort}$*, amount of cortisol-induced G-CSF release; *$t_{1/2}$ cort*, half-life of cortisol-induced G-CSF release; *BSV*, between subject variability; *CV%*, coefficient of variation; *RSE*, relative standard error obtained by nonparametric bootstrap procedure ($n = 40$)

[a] $MMT_{docetaxel}$ (h) = MMT_{FEC}*(1- $\theta_{MMT\text{-}doce}$) = 133 h

[b] Common BSV parameter for epirubicin and 4-hydroxy cyclophosphamide

docetaxel. The present study demonstrates that endogenous G-CSF concentrations are inversely related to ANC following both types of chemotherapies. An extra surge in G-CSF concentration was observed immediately following administration of high dose betamethasone prior to docetaxel administration, which subsequently translated into a temporary increase in ANC. High variability in endogenous G-CSF concentrations was observed between patients but also between treatment cycles within a patient.

These results are in line with studies in patients with hematological diseases following high dose chemotherapy where endogenous G-CSF concentrations and the inverse correlation to ANC has been reported (7, 37, 38). Since malignant neutrophils may display other properties than normal cells, potentially, the relationship between G-CSF and neutrophils could have been different in patients with solid tumors.

An integrated semi-mechanistic G-CSF-myelosuppression model including control mechanisms was developed to characterize the interaction between G-CSF and ANC. In addition the effect of high dose betamethasone administrated prior to docetaxel dosing was incorporated into the model using an empirical function. The final model successfully captured both the initial rise in endogenous G-CSF levels following chemotherapy-induced neutropenia and the subsequent return to baseline for both G-CSF and ANC and confirm the self-regulatory properties of the system. It follows that the between and within subject variability in G-CSF was to a large extent explained by the neutrophil-dependent elimination. A few patients showed however unusually high G-CSF concentrations overall or in a specific treatment cycle that may be due to increased G-CSF production in these patients, which was not accounted for in the model (see paragraph regarding inflammation markers below) and may partly lead to inflated variability in $GCSF_0$ and k_{ANC}.

At high doses of recombinant G-CSF, the neutrophil-dependent elimination of G-CSF has been reported to be saturated (15–17, 39) and G-CSF concentrations of 750-4,092 ng/L have been estimated to result in half of the maximum elimination capacity. In the present study, the maximum measured concentrations of endogenous G-CSF concentrations were <500 ng/L in 80% of the total treatment cycles (median 200 ng/L, range 5–2,133 ng/L) which is far below the concentrations reached following administration with a normal dose of recombinant G-CSF (>10 000 ng/L given 5 μg/kg filgrastim s.c (17)). It is therefore not surprising,

that the data did not support estimation of a non-linear function for the ANC-dependent elimination and that the ANC-dependent elimination rate constant for G-CSF was found to be independent of G-CSF concentration within the observed concentration range. The non-specific elimination of G-CSF was here estimated to be higher (0.59 h^{-1}) than the previously reported values of 0.15–0.38 h^{-1} following recombinant G-CSF in healthy volunteers (12, 14, 15, 17, 40–42), and in patients after high dose chemotherapy and bone marrow transplantation (43, 44). The relative contribution of the ANC-dependent elimination pathway to the total elimination of G-CSF was at baseline (ANC = 3.5•10^9 cells/L) and at nadir (ANC = 0.1•10^9 cells/L) predicted to be 97 and 49%, respectively.

The time-course of ANC was adequately described using a semi-mechanistic model where feedback mechanisms of G-CSF regulated the neutrophil production and maturation in bone marrow. The estimated model parameters were in line with reported values of the semi-mechanistic myelosuppression model for these chemotherapy treatments (27).

The reduction of ANC, following a range of various chemotherapy treatments (both mono and combination therapies), has previously been described by a semi-mechanistic model of myelosuppression as proposed by Friberg *et al.* (11) or with minor modifications (29, 30). Nevertheless, this is the first study where myelosuppression following two different drug regimens given sequentially to the same patient has been characterized using a semi-mechanistic myelosuppression model. Although the myelosuppression model has provided similar system-related parameters following various chemotherapy treatments a shorter MMT has been estimated following docetaxel treatment compared to other chemotherapies (11, 27). In our study, the nadir occurred around day 9 following docetaxel treatment, compared to day 14 following FEC treatment, and to capture the earlier nadir a shorter MMT was required and could not be explained by differences in G-CSF response or in pre-treatment with betamethasone. The lack of effect by corticosteroids is supported by early phase I studies of docetaxel, where no glucocorticoid treatment was given routinely, which reports a median time to nadir of 8 days (45–48). Thus the underlying physiological reason to the observed difference in maturation time between docetaxel and FEC remains unknown but may be due to differences in drug sensitivity of the various stages of proliferative cells in the bone marrow by the two drugs; where a later nadir would indicate earlier precursor cells being primarily affected and an earlier nadir would indicate that also cells later

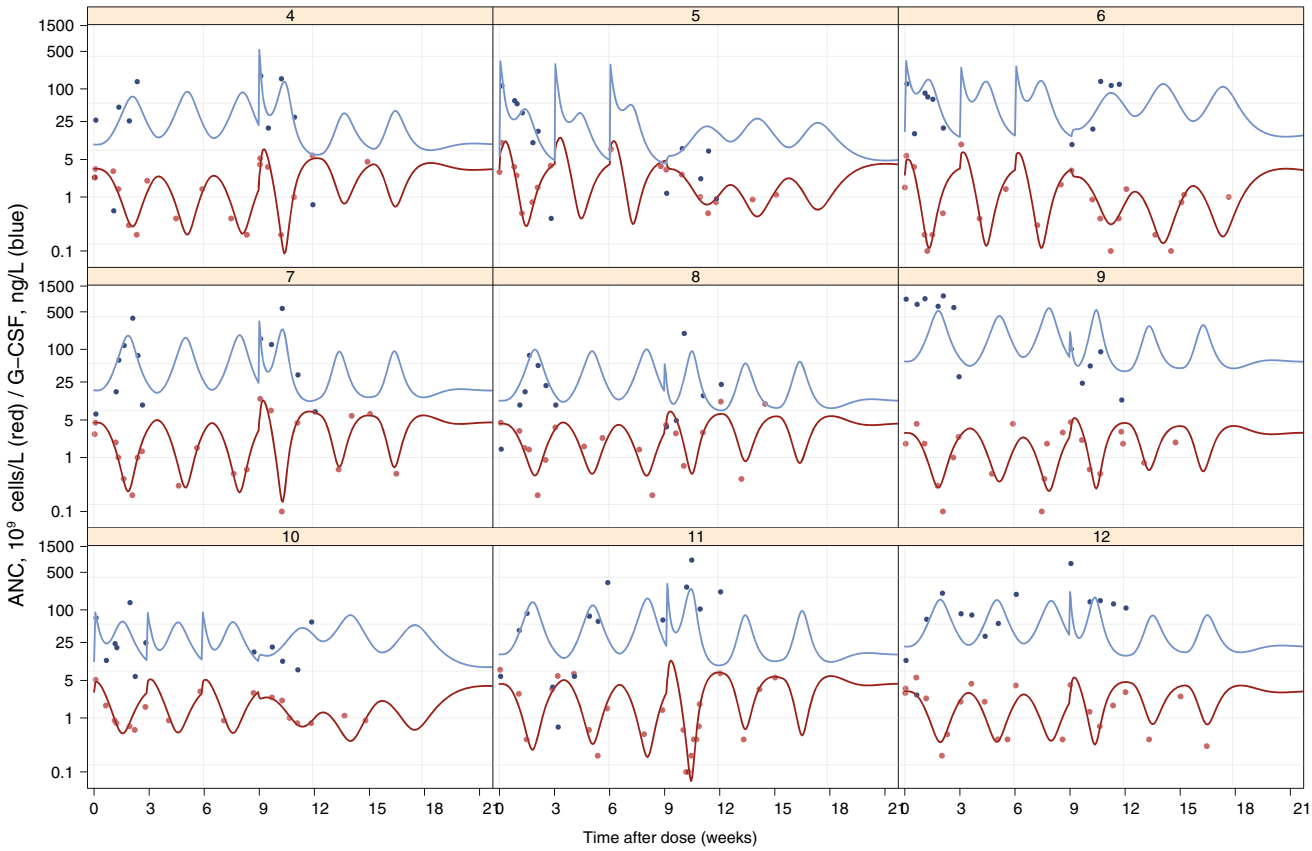

Fig 5 Individual predicted (solid lines) and observed individual (dots) endogenous G-CSF concentrations (*blue*) and ANC (*red*) for 9 patients included in the study. ID 5, 6 and 10 received docetaxel during the first three courses and FEC during the following three courses, while the other patients received the treatments in opposite order.

in the maturation chain being affected by the drug as the effect appears sooner.

A limitation of the present study was the lack of individual PK data of the chemotherapeutic drugs, which may lead to inflation of the estimated between-subject variability in drug effect as it includes both PK and PD variability; however the estimated between-subject variability for epirubicin and 4-hydroxy cyclophosphamide were relatively low compared to reported values (27, 29). Additionally, previous publications supports that variability in PK of chemotherapies has limited influence on the overall population variability in neutrophil count as demonstrated by: the estimated variability in docetaxel effect on ANC was similar in patients without PK data (41%) (27) as in patients with PK data (47%) (29); dose adjustment based on individual docetaxel clearance resulted in similar distribution of neutropenia as standard body-surface area adjusted dosing of docetaxel in patients with normal liver function (49); dose adjustment based on individual PK (therapeutic drug monitoring) was inferior to and had no additional benefit over model-based dose adjustment guided by ANC measurements (50).

A second constraint of the model is the empirical implementation of the effect of glucocorticoids on G-CSF. The current study was not designed to capture the effect of glucocorticoid; therefore, no G-CSF or ANC data was collected during the first days of each treatment cycle when betamethasone was administrated and an anticipated increase in G-CSF and ANC would have been observed (30, 32, 33, 51, 52), neither was information of time, dosing and drug concentration of betamethasone collected. Consequently, a more mechanistic model to describe the effect of glucocorticoids was not supported by the data. The same approach has previously been applied to capture the effects of corticoids on ANC (30, 31). To appropriately capture the interaction between glucocorticoids, G-CSF and ANC future studies where the appropriate information is collected are warranted.

The developed model describes the endogenous G-CSF system and provides valuable knowledge and a foundation for the understanding of rh-G-CSF therapy in combination with chemotherapy in patients. Nevertheless, given that the saturation point of the ANC-dependent elimination of G-CSF could not be estimated, the model should be used with caution when applied to doses of rh-G-CSF that would exceed the observed G-CSF concentrations in this study. Expansion of the model with data from patients following administration of recombinant G-CSF will provide a more comprehensive depiction.

In the future, patient characteristics, laboratory values and co-medications may be evaluated for impact on drug action, G-CSF and/or ANC response and may assist in identification of patients at high risk of severe neutropenia and may thus benefit from rh-G-CSF. Further, the suggested role of inflammation markers, such as AAG, interleukin 6 (IL-6) and C-reactive protein (CRP) in the regulation of G-CSF and ANC following chemotherapy (6, 37, 53, 54) remains to be elucidated. These variables may provide insights to the between and within subject variability in G-CSF not explained by changes in neutrophil count, including why some patients had extremely elevated G-CSF concentrations before the first chemotherapy dose (e.g. patient 9 in Fig. 5). Furthermore, elevated levels of IL-6 and CRP have been reported in patients experiencing febrile neutropenia and thus may be of predictive importance.

In conclusion, this study supported the hypothesis that endogenous G-CSF concentrations are inversely correlated with ANC following chemotherapy in patients with early breast cancer and that G-CSF is primarily cleared from the blood by ANC. The high variability observed in G-CSF concentrations between and within subjects was to a large extent explained by the neutrophil-dependent elimination. The model was also able to capture the early increased release of G-CSF by high dose glucocorticoid prior to docetaxel administration in breast cancer patients that has earlier been observed in healthy volunteers. The model may be a useful tool in further characterization of the biological system and in optimization of chemotherapy treatments.

ACKNOWLEDGMENTS AND DISCLOSURES

We are grateful to all the patients who kindly participated in the study. We also like to thank Anders Larsson, Åsa Hedlund and Jessica Barrefjord for technical assistance. Model estimation was in part performed on resources provided by Swedish National Infrastructure for Computing (SNIC) through Uppsala Multidisciplinary Center for Advanced Computational Science (UPPMAX). Martin Agback at UPPMAX is acknowledged for assistance concerning technical aspects in making NONMEM run on the UPPMAX resources. The study was supported by the Swedish Cancer Society.

REFERENCES

1. Crawford J, Dale DC, Kuderer NM, Culakova E, Poniewierski MS, Wolff D, *et al.* Risk and timing of neutropenic events in adult cancer patients receiving chemotherapy: the results of a prospective nationwide study of oncology practice. J Natl Compr Cancer Netw JNCCN. 2008;6(2):109–18.
2. Lyman GH, Dale DC, Friedberg J, Crawford J, Fisher RI. Incidence and predictors of low chemotherapy dose-intensity in aggressive non-Hodgkin's lymphoma: a nationwide study. J Clin Oncol Off J Am Soc Clin Oncol. 2004;22(21):4302–11.
3. Colleoni M, Price K, Castiglione-Gertsch M, Goldhirsch A, Coates A, Lindtner J, *et al.* Dose–response effect of adjuvant

cyclophosphamide, methotrexate, 5-fluorouracil (CMF) in node-positive breast cancer. International Breast Cancer Study Group. Eur J Cancer Oxf Engl 1990. 1998 Oct;34(11):1693–700.
4. Nicola NA. Granulocyte colony-stimulating factor. Immunol Ser. 1990;49:77–109.
5. Roberts AW. G-CSF: a key regulator of neutrophil production, but that's not all! Growth Factors Chur Switz. 2005;23(1):33–41.
6. Hareng L, Hartung T. Induction and regulation of endogenous granulocyte colony-stimulating factor formation. Biol Chem. 2002;383(10):1501–17.
7. Reisbach G, Kamp T, Welzl G, Geiz C, Abedinpour F, Lodri A, *et al.* Regulated plasma levels of colony-stimulating factors, interleukin-6 and interleukin-10 in patients with acute leukaemia and non-hodgkin's lymphoma undergoing cytoreductive chemotherapy. Br J Haematol. 1996;92(4):907–12.
8. Kawakami M, Tsutsumi H, Kumakawa T, Abe H, Hirai M, Kurosawa S, *et al.* Levels of serum granulocyte colony-stimulating factor in patients with infections. Blood. 1990;76(10):1962–4.
9. Friberg LE, Karlsson MO. Mechanistic models for myelosuppression. Invest New Drugs. 2003;21(2):183–94.
10. Soto E, Staab A, Doege C, Freiwald M, Munzert G, Trocóniz IF. Comparison of different semi-mechanistic models for chemotherapy-related neutropenia: application to BI 2536 a Plk-1 inhibitor. Cancer Chemother Pharmacol. 2011;68(6):1517–27.
11. Friberg LE, Henningsson A, Maas H, Nguyen L, Karlsson MO. Model of chemotherapy-induced myelosuppression with parameter consistency across drugs. J Clin Oncol Off J Am Soc Clin Oncol. 2002;20(24):4713–21.
12. Hayashi N, Kinoshita H, Yukawa E, Higuchi S. Pharmacokinetic and pharmacodynamic analysis of subcutaneous recombinant human granulocyte colony stimulating factor (lenograstim) administration. J Clin Pharmacol. 1999;39(6):583–92.
13. Krzyzanski W, Ramakrishnan R, Jusko WJ. Basic pharmacodynamic models for agents that alter production of natural cells. J Pharmacokinet Biopharm. 1999;27(5):467–89.
14. Sugiura M, Yamamoto K, Sawada Y, Iga T. Pharmacokinetic/pharmacodynamic analysis of neutrophil proliferation induced by recombinant granulocyte colony-stimulating factor (rhG-CSF): comparison between intravenous and subcutaneous administration. Biol Pharm Bull. 1997;20(6):684–9.
15. Wang B, Ludden TM, Cheung EN, Schwab GG, Roskos LK. Population pharmacokinetic-pharmacodynamic modeling of filgrastim (r-metHuG-CSF) in healthy volunteers. J Pharmacokinet Pharmacodyn. 2001;28(4):321–42.
16. Roskos LK, Lum P, Lockbaum P, Schwab G, Yang B-B. Pharmacokinetic/pharmacodynamic modeling of pegfilgrastim in healthy subjects. J Clin Pharmacol. 2006;46(7):747–57.
17. Krzyzanski W, Wiczling P, Lowe P, Pigeolet E, Fink M, Berghout A, *et al.* Population modeling of filgrastim PK-PD in healthy adults following intravenous and subcutaneous administrations. J Clin Pharmacol. 2010;50(9 Suppl):101S–12.
18. Sugiura M, Ohno Y, Yamada Y, Suzuki H, Iga T. Pharmacokinetic/pharmacodynamic analysis of neutrophil proliferation induced by rhG-CSF in patients receiving antineoplastic drugs. Yakugaku Zasshi. 2004;124(9):599–604.
19. Pastor ML, Laffont CM, Gladieff L, Schmitt A, Chatelut E, Concordet D. Model-Based Approach to Describe G-CSF Effects in Carboplatin-Treated Cancer Patients. Pharm Res. 2013 Jun 26
20. Yang B-B, Lum PK, Hayashi MM, Roskos LK. Polyethylene glycol modification of filgrastim results in decreased renal clearance of the protein in rats. J Pharm Sci. 2004;93(5):1367–73.
21. Roskos LK, Cheung EN, Vincent M, Foote M, Morstyn G. Pharmacology of filgrastim (r-metHuG-CSF). Filgrastim R-MetHuG-CSF Clin Pract N Y NY Marcel Dekker. 1998;41–9.
22. Cockcroft DW, Gault MH. Prediction of creatinine clearance from serum creatinine. Nephron. 1976;16(1):31–41.
23. Bruno R, Vivier N, Vergniol JC, De Phillips SL, Montay G, Sheiner LB. A population pharmacokinetic model for docetaxel (Taxotere): model building and validation. J Pharmacokinet Biopharm. 1996;24(2):153–72.
24. Sandström M, Lindman H, Nygren P, Johansson M, Bergh J, Karlsson MO. Population analysis of the pharmacokinetics and the haematological toxicity of the fluorouracil-epirubicin-cyclophosphamide regimen in breast cancer patients. Cancer Chemother Pharmacol. 2006;58(2):143–56.
25. Urien S, Rezaí K, Lokiec F. Pharmacokinetic modelling of 5-FU production from capecitabine–a population study in 40 adult patients with metastatic cancer. J Pharmacokinet Pharmacodyn. 2005;32(5–6):817–33.
26. Smith C, Beutler E, Lichtman M, Coller B, Kipps T. Williams hematology. Lichtman M Kipps T Seligsohn U Kaushansky K JT P Eds. 2010;
27. Hansson EK, Wallin JE, Lindman H, Sandström M, Karlsson MO, Friberg LE. Limited inter-occasion variability in relation to inter-individual variability in chemotherapy-induced myelosuppression. Cancer Chemother Pharmacol. 2010;65(5):839–48.
28. Gisleskog PO, Karlsson MO, Beal SL. Use of prior information to stabilize a population data analysis. J Pharmacokinet Pharmacodyn. 2002;29(5–6):473–505.
29. Quartino AL, Friberg LE, Karlsson MO. A simultaneous analysis of the time-course of leukocytes and neutrophils following docetaxel administration using a semi-mechanistic myelosuppression model. Invest New Drugs. 2012;30(2):833–45.
30. Ozawa K, Minami H, Sato H. Population pharmacokinetic and pharmacodynamic analysis for time courses of docetaxel-induced neutropenia in Japanese cancer patients. Cancer Sci. 2007;98(12):1985–92.
31. Soto E, Staab A, Freiwald M, Munzert G, Fritsch H, Döge C, *et al.* Prediction of neutropenia-related effects of a new combination therapy with the anticancer drugs BI 2536 (a Plk1 Inhibitor) and pemetrexed. Clin Pharmacol Ther. 2010;88(5):660–7.
32. Czerwinski AW, Czerwinski AB, Whitsett TL, Clark ML. Effects of a single, large, intravenous injection of dexamethasone. Clin Pharmacol Ther. 1972;13(5):638–42.
33. Mager DE, Lin SX, Blum RA, Lates CD, Jusko WJ. Dose equivalency evaluation of major corticosteroids: pharmacokinetics and cell trafficking and cortisol dynamics. J Clin Pharmacol. 2003;43(11):1216–27.
34. Friberg LE, Brindley CJ, Karlsson MO, Devlin AJ. Models of schedule dependent haematological toxicity of 2'-deoxy-2'-methylidenecytidine (DMDC). Eur J Clin Pharmacol. 2000;56(8):567–74.
35. Karlsson MO, Port RE, Ratain MJ, Sheiner LB. A population model for the leukopenic effect of etoposide. Clin Pharmacol Ther. 1995;57(3):325–34.
36. Beal S, Sheiner L, Boeckmann A, Bauer R. NONMEM User's Guides (1989–2009). 2009. Icon Dev Solut Ellicott City MD.
37. Saito S, Kawano Y, Watanabe T, Okamoto Y, Abe T, Kurada Y, *et al.* Serum granulocyte colony-stimulating factor kinetics in children receiving intense chemotherapy with or without stem cell support. J Hematother. 1999;8(3):291–7.
38. Takatani H, Soda H, Fukuda M, Watanabe M, Kinoshita A, Nakamura T, *et al.* Levels of recombinant human granulocyte colony-stimulating factor in serum are inversely correlated with circulating neutrophil counts. Antimicrob Agents Chemother. 1996;40(4):988–91.
39. Kuwabara T, Kobayashi S, Sugiyama Y. Pharmacokinetics and pharmacodynamics of a recombinant human granulocyte colony-stimulating factor. Drug Metab Rev. 1996;28(4):625–58.
40. Kuwabara T, Kobayashi S, Sugiyama Y. Kinetic analysis of receptor-mediated endocytosis of G-CSF derivative, nartograstim, in rat bone marrow cells. Am J Physiol. 1996;271(1 Pt 1):E73–84.

41. Wiczling P, Lowe P, Pigeolet E, Lüdicke F, Balser S, Krzyzanski W. Population pharmacokinetic modelling of filgrastim in healthy adults following intravenous and subcutaneous administrations. Clin Pharmacokinet. 2009;48(12):817–26.
42. Watari K, Ozawa K, Takahashi S, Tojo A, Tani K, Kamachi S, *et al*. Pharmacokinetic studies of intravenous glycosylated recombinant human granulocyte colony-stimulating factor in various hematological disorders: inverse correlation between the half-life and bone marrow myeloid cell pool. Int J Hematol. 1997;66(1):57–67.
43. Fukuda M, Oka M, Ishida Y, Kinoshita H, Terashi K, Fukuda M, *et al*. Effects of renal function on pharmacokinetics of recombinant human granulocyte colony-stimulating factor in lung cancer patients. Antimicrob Agents Chemother. 2001;45(7):1947–51.
44. Stute N, Santana VM, Rodman JH, Schell MJ, Ihle JN, Evans WE. Pharmacokinetics of subcutaneous recombinant human granulocyte colony-stimulating factor in children. Blood. 1992;79(11):2849–54.
45. Extra J-M, Rousseau F, Bruno R, Clavel M, Bail NL, Marty M. Phase I and pharmacokinetic study of taxotere (RP 56976; NSC 628503) given as a short intravenous infusion. Cancer Res. 1993;53(5):1037–42.
46. Cortes JE, Pazdur R. Docetaxel. J Clin Oncol. 1995;13(10):2643–55.
47. Burris H, Irvin R, Kuhn J, Kalter S, Smith L, Shaffer D, *et al*. Phase I clinical trial of taxotere administered as either a 2-hour or 6-hour intravenous infusion. J Clin Oncol. 1993;11(5):950–8.
48. Tomiak E, Piccart M, Kerger J, Lips S, Awada A, De Valeriola D, *et al*. Phase I study of docetaxel administered as a 1-hour intravenous infusion on a weekly basis. J Clin Oncol. 1994;12(7):1458–67.
49. Quartino AL. Pharmacometric models for improved prediction of myelosuppression and treatment response in oncology [internet]. Uppsala: Acta Universitatis Upsaliensis; 2011. Available from: http://urn.kb.se/resolve?urn=urn:nbn:se:uu:diva-150431.
50. Wallin JE, Friberg LE, Karlsson MO. Model-based neutrophil-guided dose adaptation in chemotherapy: evaluation of predicted outcome with different types and amounts of information. Basic Clin Pharmacol Toxicol. 2010;106(3):234–42.
51. Wakayama T, Sohmiya M, Furuya H, Murakami Y, Kato Y. Increased serum human granulocyte colony-stimulating factor (G-CSF) levels following intravenous infusion of high-dose methylprednisolone. Endocr J. 1996;43(1):67–72.
52. Jilma B, Stohlawetz P, Pernerstorfer T, Eichler HG, Müllner C, Kapiotis S. Glucocorticoids dose-dependently increase plasma levels of granulocyte colony stimulating factor in man. J Clin Endocrinol Metab. 1998;83(3):1037–40.
53. Dexter TM, Simmons P, Purnell RA, Spooncer E, Schofield R. The regulation of hemopoietic cell development by the stromal cell environment and diffusible regulatory molecules. Prog Clin Biol Res. 1984;148:13–33.
54. Dexter TM. Regulation of hemopoietic cell growth and development: experimental and clinical studies. Leukemia. 1989;3(7):469–74.